TRIDIMENSIONAL FLOW SIMULATION WITH FINITE ELEMENTS STABILIZED BY CBS SCHEME

Gustavo Aparecido Pita Baggio

João Batista Campos Silva

gapbaggio@dem.feis.unesp.br

jbcampos@ dem.feis.unesp.br

Universidade Estadual Paulista - UNESP

Avenida Brasil, nº56, 15385-000, Ilha Solteira, São Paulo, Brasil.

Abstract. *This paper presents computational results of incompressible steady flows simulations by solving the Navier-Stokes equations using a finite element method combined with the characteristic based split scheme (CBS). The classical finite element method called Bubnov-Galerkin or Galerkin Method (FEM) is considered the best method for solving purely diffusion problems, however, in case of problems with convection dominant as in many problems of fluid flows, the FEM produces oscillating solutions for high Reynolds numbers. The main goal of this work is to highlight the simulation method and the results of some common tridimensional problems used for code validation and verification. The results show great agreement with literature.*

Keywords: *Steady flow, Finite elements, Artificial compressibility, CBS.*

1 INTRODUCTION

The standard Galerkin finite element method (FEM) gives the minimum error in the L2 norm for self-adjoint problems and results in a symmetric algebraic system of equations. However, the main equations that rule the fluid dynamics are non-self-adjoint equations and if the FEM is used to solve them, without any stabilization, it may result in several oscillations. The instabilities in the solution, generally, originate if some care is not taken in the discretization of the non-linear convective acceleration terms. The convective terms, also, make the equations non-self-adjoint, and after discretization the resulting algebraic system of equations isn't symmetric (Liu, 2005).

One way to remedy or reduce this kind of instabilities of the solution is to apply upwind discretization techniques to the convective terms, which are the main source of oscillations when solving this kind of problem. For stabilization via transient formulations, there is the Characteristic-Galerkin, (Nithiarasu et al., 2005), (Zienkiewicz et al., 1999) and (Zienkiewicz e Taylor, 2000) which is the category that the CBS scheme belongs to.

Also, instabilities can appear if in the incompressible limit, the Ladyshenskaya-Babuska-Brezzi (LBB) condition is not respected. The violation of this condition often results in numerically unphysical oscillations and it is related to the order of the interpolation functions used for velocity and pressure fields (Liu, 2005). In the FEM, generally, the pressure field is interpolated by functions one order bellow the order of the interpolation functions to the velocity field.

In order to apply the Characteristic-Galerkin approach to the momentum equations, firstly, the pressure term is dropped out and a moving coordinate system is assumed, like in a Lagrangian fluid dynamics approach. Although this approach eliminates the convection term responsible for spatial oscillation when discretized in space, it introduces the complication of a moving coordinate system. However, a simple expansion in Taylor series in space avoids such a moving coordinate approach. So, we are able to calculate an intermediate velocity field and this is the first step of CBS scheme. In a second step, the pressure field is calculated with an artificial compressibility method. Then, in a third step, the intermediate velocities will be corrected. With the corrected velocities in hand, in the last step we can calculate any additional scalar variables with the appropriate governing equation. Owing to the split introduced in the equations, the method is referred as the Characteristic Based Split (CBS) scheme, (Lewis et al., 2004).

The CBS scheme for compressible and incompressible flow problems was first introduced into the finite element literature in 1995 by Zienkiewicz and Codina and co-workers. Since its introduction to the computational and numerical methods community, the CBS scheme has received great interest and has been subject of study for several researchers for both incompressible and compressible flows (Liu, 2005).

In this work, we use a fully explicit AC-CBS scheme to solve a tridimensional incompressible steady flow in a cubic cavity, flow around a cylinder and flow around a sphere. Another objective of the work is to learning some aspects of implementation of the FEM-CBS in order to simulate transient flow problems. The Reynolds numbers considered are from low to moderate range in order to keep within the laminar flow range, because no turbulence model is used and thereby ensure that the results obtained will have a physically expected behavior.

2 GOVERNING EQUATIONS

The governing equations of the problem are the continuity equation, the tridimensional Navier-Stokes equations. For forced convection problems, these equations are commonly non-dimensionalized and they form the following set of equations.

$$\frac{1}{c^{*2}}\frac{\partial p^*}{\partial t^*} \approx \frac{\partial \rho^*}{\partial t^*} = \frac{\partial U_i^*}{\partial x_i^*} \tag{1}$$

$$\frac{\partial U_i^*}{\partial t^*} + \frac{\partial\left(u_j^* U_i^*\right)}{\partial x_j^*} = -\frac{\partial p^*}{\partial x_i^*} + \frac{\partial}{\partial x_j^*}\left(\frac{1}{\mathrm{Re}}\frac{\partial u_i^*}{\partial x_j^*}\right) \tag{2}$$

2.1 The Characteristic Galerkin.

Now, the Characteristic Galerkin (CG) procedure will be described for a simple 1D convection-diffusion equation for simplicity. Consider the following transport equation for a scalar variable:

$$\frac{\partial \phi}{\partial t} + u_1\frac{\partial \phi}{\partial x_1} - \frac{\partial}{\partial x_1}\left(k\frac{\partial \phi}{\partial x_1}\right) + Q = 0 \tag{3}$$

The Characteristic Galerkin is based on evaluation of the time derivative along the characteristic that eliminate the convective term in the transport equation (as in a Lagrangian fluid dynamics approach). So, the Eq. (3) is now:

$$\frac{\partial \phi}{\partial t}\left(x_1^{'}, t\right) - \frac{\partial}{\partial x_1^{'}}\left(k\frac{\partial \phi}{\partial x_1^{'}}\right) = 0 \tag{4}$$

Here, although this approach eliminates the convection term responsible for spatial oscillation when discretized in space, the complication of a moving coordinate system is introduced. It is worth to say that Eq. (4) is a self-adjoint equation.

In order to solve the problem of a moving coordinate system, a simple expansion in Taylor series is used and the Eq. (4), in the semi-discrete form, turns to Eq. (5).

$$\frac{\phi^{n+1} - \phi^n}{\Delta t} = -u_1\frac{\partial \phi^n}{\partial x_1} + u_1^2\frac{\Delta t}{2}\frac{\partial^2 \phi^n}{\partial x_1^2} + \frac{\partial}{\partial x_1}\left(k\frac{\partial \phi}{\partial x_1}\right)^n \tag{5}$$

At this point, we get to the end of the Characteristic Galerkin procedure and the Eq. (5) is ready for spatial discretization. In this work, the FEM is used to spatial discretization. Once FEM is used, before proceed with the integration, we must apply Green’s lemma to some of the integrals in order to get the weak formulation. For a 3D convection-diffusion equation, after the Characteristic Galerkin and the FEM procedures have been applied, we get the Eq. (6).

$$\int_{\Omega}[N]^T[N]d\Omega\frac{\{\phi\}^{n+1}-\{\phi\}^n}{\Delta t}=-u_i\int_{\Omega}[N]^T\frac{\partial[N]}{\partial x_i}d\Omega\{\phi\}^n-\int_{\Omega}\frac{\partial[N]^T}{\partial x_i}k_i\frac{\partial[N]}{\partial x_i}d\Omega\{\phi\}^n+$$
$$+\int_{\Gamma}[N]^Tk_i\frac{\partial[N]}{\partial x_i}n_i d\Gamma\{\phi\}^n-\frac{\Delta t}{2}u_k u_j\left[\int_{\Omega}\frac{\partial[N]^T}{\partial x_k}\frac{\partial[N]}{\partial x_j}d\Omega\{\phi\}^n+\int_{\Gamma}[N]^T\frac{\partial[N]}{\partial x_j}n_k d\Gamma\{\phi\}^n\right] \tag{6}$$

Where n_i is the direction cosines of the outward normal $\boldsymbol{n}$, Ω is the domain and Γ is the contour of the domain. The Characteristic Galerkin procedure and the FEM discretization are described with more details in Zienkiewicz et al., (2014).

2.2 The Characteristic Based Split.

The application of the CBS scheme for flow equations involves the discretization of the time derivative in steps. Just for remember, as shown in the previous section, the CG procedure is the first step of CBS and we are able to calculating an intermediary velocity field, since the pressure terms be removed from N-S equations, fact that leads to the need of an 'adjust', which happens in the following steps of CBS scheme. In the second step, the pressure field is calculated from a Poisson equation in a scheme known as semi-implicit (Nithiarasu et. al., 2005). However, the semi-implicit method leads us to the need of a linear system solution in each time step and it has an expensive computational cost for tridimensional cases. It can be avoided with a fully explicit scheme using an artificial compressibility method.

With the pressure field in hands, the third step of the CBS scheme is to correct the intermediary velocity field calculated in the first step.

2.3 Artificial Compressibility.

The artificial compressibility method can be employed to eliminate the restrictions posed by the speed of sound at pressure calculation by taking an artificial value for the speed of sound which is sufficiently low. This is only possible if steady state condition exists.

$$\frac{\Delta\rho}{\Delta t}=\left(\frac{1}{c^2}\right)^n\frac{\Delta p}{\Delta t}\approx\left(\frac{1}{\beta^2}\right)^n\frac{\Delta p}{\Delta t}=-\left[\frac{\partial\tilde{u}_i^n}{\partial x_i}-\Delta t\left(\frac{\partial^2 p^n}{\partial x_i\partial x_i}\right)\right] \tag{7}$$

where β is an artificial parameter with velocity dimension. This parameter may be either given as a constant or determined based on diffusive (u_{diff}) or convective (u_{conv}) time step restrictions. So, the value of β may be locally calculated using the following relation:

$$\beta = \left(C_0, u_{diff}, u_{conv}\right) \tag{8}$$

where:

$$u_{conv} = |\mathrm{u}| = \sqrt{u_i u_i} \tag{9}$$

and:

$$u_{diff} = \frac{\nu}{h} \tag{10}$$

where C_0 is a small constant, h is the element size and ν is the kinematic viscosity of the fluid.

The following summarizes the main steps for the time discretization of the equations that make up the CBS scheme with artificial compressibility:

Step 1: Intermediate velocity field

$$\frac{\tilde{u}_i - u_i^n}{\Delta t} = -u_j \frac{\partial u_i^n}{\partial x_j} + \nu \left(\frac{\partial^2 u_i}{\partial x_j^2}\right)^n + u_k \frac{\Delta t}{2} \frac{\partial}{\partial x_k}\left[u_j \frac{\partial u_i}{\partial x_j}\right]^n \tag{11}$$

Step 2: Pressure Calculation

$$\left(\frac{1}{\beta^2}\right)^n \frac{\Delta p}{\Delta t} = -\left[\frac{\partial \tilde{u}_i^n}{\partial x_i} - \Delta t \left(\frac{\partial^2 p^n}{\partial x_i \partial x_i}\right)\right] \tag{12}$$

Step 3: Velocity Correction

$$\frac{u_i^{n+1} - \tilde{u}_i}{\Delta t} = -\frac{\partial p^n}{\partial x_i} + u_k \frac{\Delta t}{2} \frac{\partial}{\partial x_k}\left(\frac{\partial p}{\partial x_i}\right)^n \tag{13}$$

Now, applying the Galerkin method for spatial discretization, the 3 steps of CBS scheme in matrix form become:

Step 1: Intermediate velocity field

$$[M]\frac{\{\Delta\tilde{u}_i\}}{\Delta t} = -[C]\{u_i\}^n - [K_m]\{u_i\}^n - [K_s]\{u_i\}^n + \{f_i\} \tag{14}$$

Step 2: Pressure Calculation

$$[M]\frac{\{\Delta p\}}{\Delta t} = -[G_i]\{\tilde{u}_i\}^n - \Delta t[H]\{p\}^n + \{f_p\} \tag{15}$$

Step 3: Velocity Correction

$$[M]\frac{\{u_i\}^{n+1} - \{\tilde{u}_i\}}{\Delta t} = -[G_i]\{p\}^n + \frac{\Delta t}{2}[P]\{p\}^n \tag{16}$$

2.4 Lumped Mass Matrix

The mass matrix [*M*] used in the above steps may be 'lumped' to simplify the solution procedure. This is an approximation, but a worthwhile and time-saving approximation. Mass lumping will eliminate the need for the matrix solution procedure necessary for consistent mass matrices.

The matrix [*M*] in Eq. (17) is the same in left side or of Eq. (6) and here is written to help us to define it.

$$\int_{\Omega}[N]^T[N]d\Omega\frac{\{\phi\}^{n+1} - \{\phi\}^n}{\Delta t} = [M_e]\frac{\{\Delta\phi\}}{\Delta t} \tag{17}$$

$$[M_e] = \int_{\Omega}\begin{bmatrix} N_1 \\ N_2 \\ N_3 \\ N_4 \end{bmatrix}\begin{bmatrix} N_1 & N_2 & N_3 & N_4 \end{bmatrix}d\Omega = \int_{\Omega}\begin{bmatrix} N_1^2 & N_1N_2 & N_1N_3 & N_1N_4 \\ N_2N_1 & N_2^2 & N_2N_3 & N_2N_4 \\ N_3N_1 & N_3N_2 & N_3^2 & N_3N_4 \\ N_4N_1 & N_4N_2 & N_4N_3 & N_4^2 \end{bmatrix}d\Omega \tag{18}$$

In the Eq. (18), the integral must be performed to finally get the mass matrix. For linear elements, one integration formula can be written as shown in Eq. (19) (Zienkiewicz et al., 2014).

$$\int_V N_1^a N_2^b N_3^c N_4^d dV = \frac{a!b!c!d!}{(a+b+c+d+3)!}6V \tag{19}$$

The lumped mass matrix for a linear tetraedral element is constructed by summing the columns and placing the sum on the diagonals. The elemental original and lumped mass matrix of a linear tetrahedral element are described in the following equations.

$$\left[M_e\right] = \int_\Omega [N]^T [N] d\Omega \quad = \frac{V}{20}\begin{bmatrix} 2 & 1 & 1 & 1 \\ 1 & 2 & 1 & 1 \\ 1 & 1 & 2 & 1 \\ 1 & 1 & 1 & 2 \end{bmatrix} \tag{20}$$

$$\left[M_{Le}\right] = \frac{V}{20}\begin{bmatrix} 5 & 0 & 0 & 0 \\ 0 & 5 & 0 & 0 \\ 0 & 0 & 5 & 0 \\ 0 & 0 & 0 & 5 \end{bmatrix} = \frac{V}{4}\begin{bmatrix} 1 & 0 & 0 & 0 \\ 0 & 1 & 0 & 0 \\ 0 & 0 & 1 & 0 \\ 0 & 0 & 0 & 1 \end{bmatrix} \tag{21}$$

If the above mass lumping procedure is introduced into the CBS steps, some small errors will occur in the transient solution but an accurate solution still can be obtained by appropriate mesh refinement. For steady state solutions, however, no errors are introduced (Lewis et al., 2004).

3 RESULTS

3.1 Flow in a Cubic Cavity

The flow in the cavity is a widely discussed issue in order to validate the results of computer codes. The geometry and the boundary conditions of this case are well-known but it can be found in Lewis et al. (2004). Despite the simple geometry, the cavity can present the most complex phenomena of a flow such as recirculation. The irregular mesh contains 19379 nodes and 97599 tetrahedral elements. These problems have been simulated by Baggio, (2015). The Figures 1 to 3 shows the results for Reynolds number equal to 100, 400 and 1000, respectively. For each one, the velocity component in x direction, in the center of the cavity ($y=0,5$ and $z=0,5$) is compared with results from Wong and Baker, (2011). We can observe a good agreement between the results for low Reynolds number, but to Reynolds number equal 1000, the differences between the may due to a lack of mesh refinement.

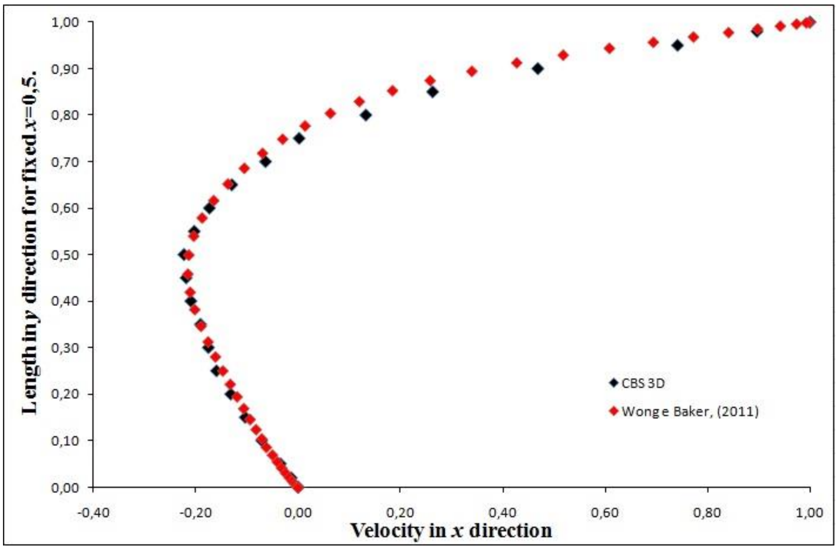

Figure 1. Results for Reynolds number equal to 100.

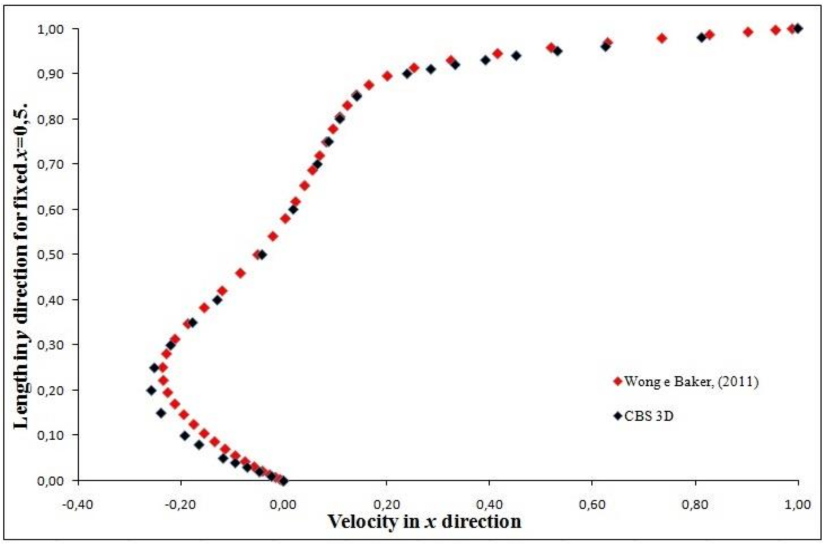

Figure 2. Results for Reynolds number equal to 400.

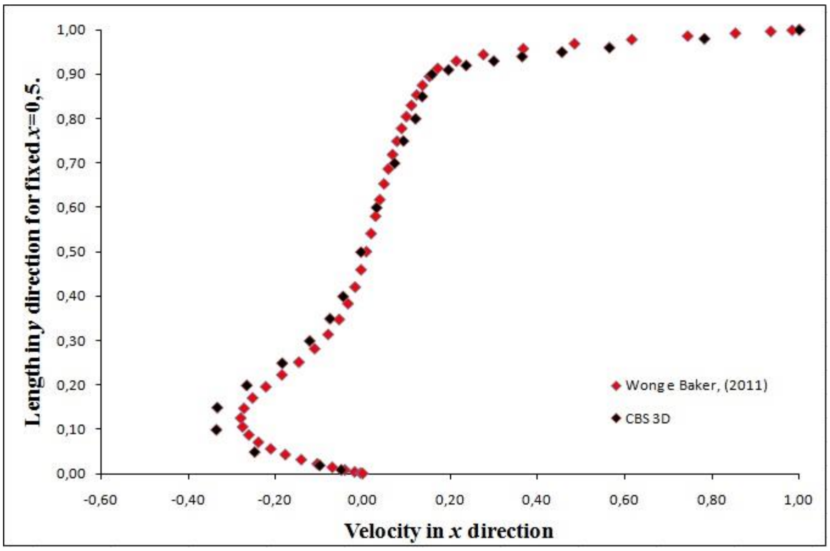

Figure 3. Results for Reynolds number equal to 1000.

3.2 Flow around a Cylinder.

This case is widely studied for computational codes validation. It can be find in many literature of computational analysis and also there are many experimental studies. Although it is a 2D case, here we are presenting a study regarding this case. The objective here is to analyze the pressure coefficient over the cylinder surface for Reynolds number equal to 40. The mesh contains 219358 nodes and 1206656 elements.

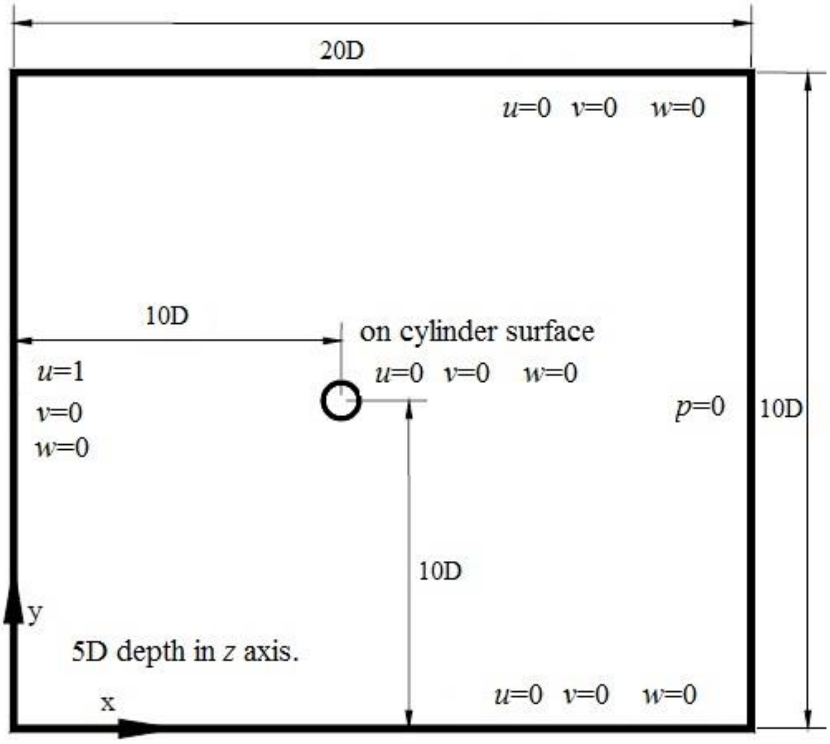

Figure 4. Geometry details and boundary conditions.

The pressure coefficient is calculated with the equation below, where p_0 is the stagnation pressure measured in front of the cylinder (θ = 0º). The pressure coefficient is calculated using the Eq. (22) and is the non-dimensional form of pressure used on governing equations.

$$c_p = p^* = \frac{p}{\frac{1}{2}\rho u_\infty^2} \tag{22}$$

The results are normalized like in the following Eq. (23) and they are plotted in Figure 5, where is presented the pressure coefficient value varying the angle θ, which is measured from the stagnation point to the rear of the cylinder. By inspection of the results, it is possible to observe the excellent agreement of them. In Figure 5 is shown the result predicted using the theory of potential flow by the continuous line.

$$C_p = 1 + p_i^* - p_0^* \tag{23}$$

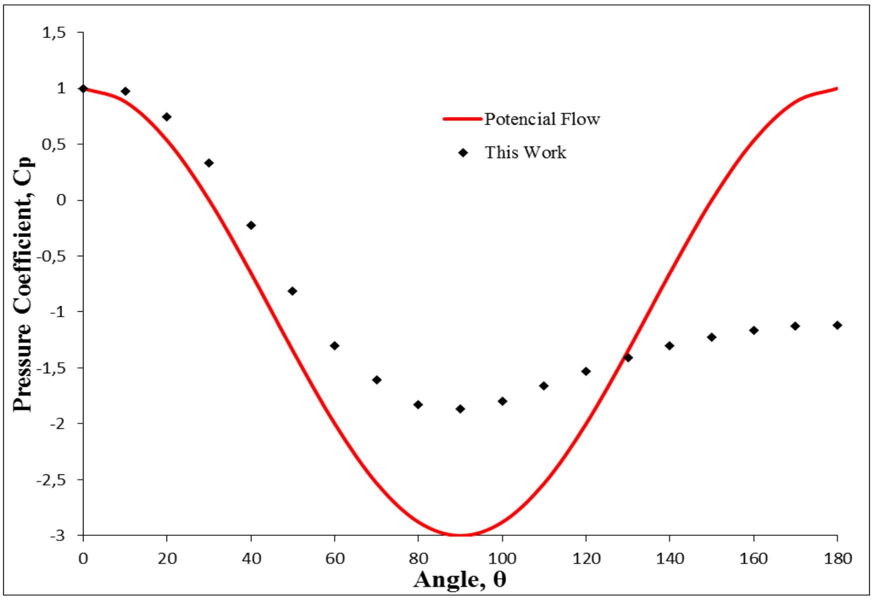

Figure 5. Pressure coefficient over the cylinder for *Re*= 40.

In Figure 6 is shown a detail of velocity magnitude around the cylinder. It is possible to observe the laminar behavior of the flow.

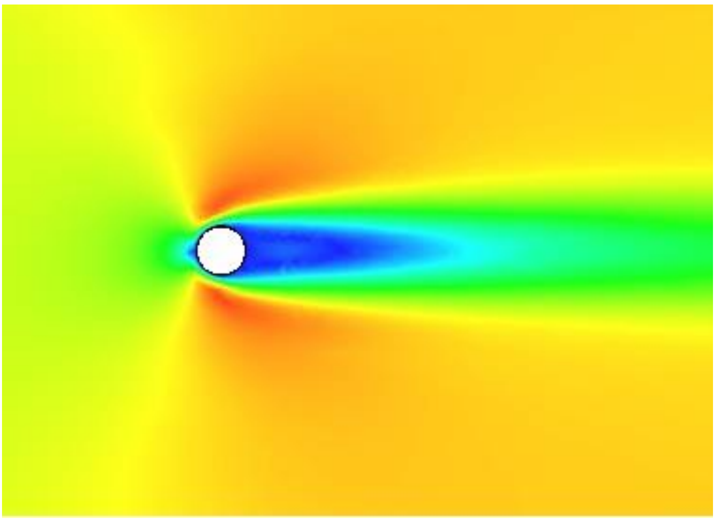

Figure 6. Velocity magnitude field for Re=40.

3.3 Flow around a Sphere.

As in previous cases, this is also a case widely studied for the computational code validation. One can find in literature many computational studies and also many experimental studies because it is a relatively easy problem to reproduce in the laboratory. Here we are presenting some studies regarding this case. This geometry is in according with the studies presented by Le Clair et al., (1970) and Campregher et al., (2009) and the objective is to compare the results of the pressure coefficient over the sphere surface and the bubble length for Reynolds number equal to 100 and 200. The mesh contains 68521 nodes and 369928 elements.

Results to the *L/D* ratio are presented in Table 1. Where *L* is the bubble length and *D* is the sphere diameter, see Figure 7.

Table 1. Results for bubble length.

Bubble Length	Re = 100	Re = 200
This Work	0,862	1,47
Fornberg (1988)	0,87	1,43
Johnson and Patel (1999)	0,88	1,45
Tomboulides and Orszag (2000)	0,87	1,43
Gilmanov et al. (2003)	0,85	1,44
Campregher et al. (2009)	0,94	1,40

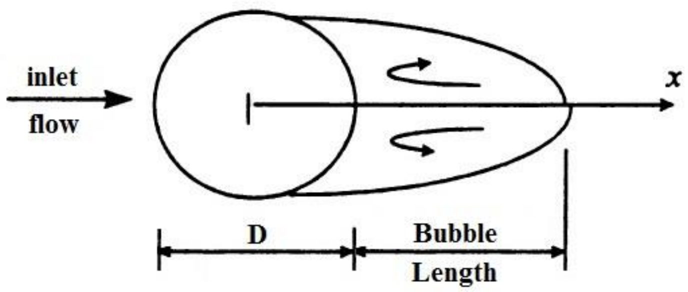

Figure 7. Flow over the sphere sketch.

Figures 8 and 9 presents the results for pressure coefficient over the sphere surface such as in the case of cylinder, see Eq. (22), but they are not normalized with Eq. (23).

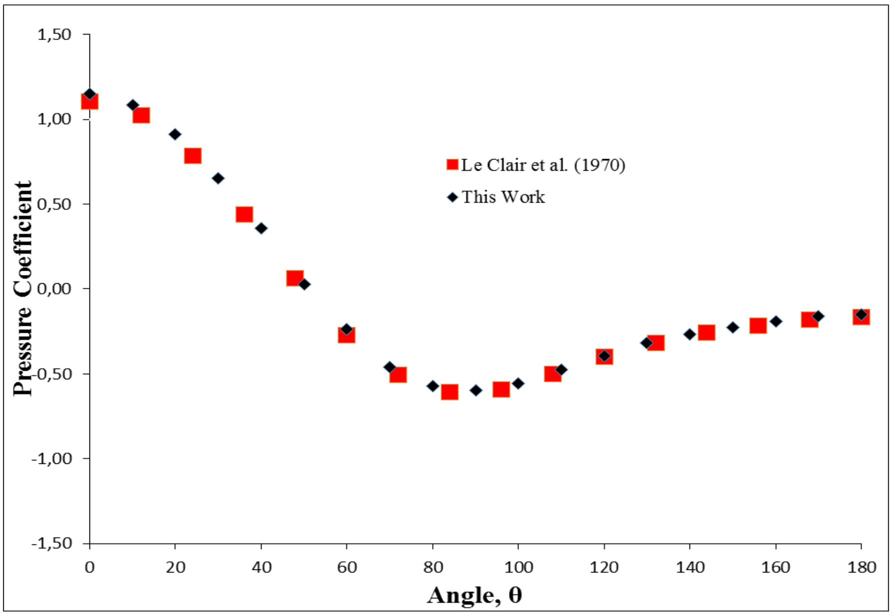

Figure 8. Pressure coefficient over the sphere surface for *Re*=100.

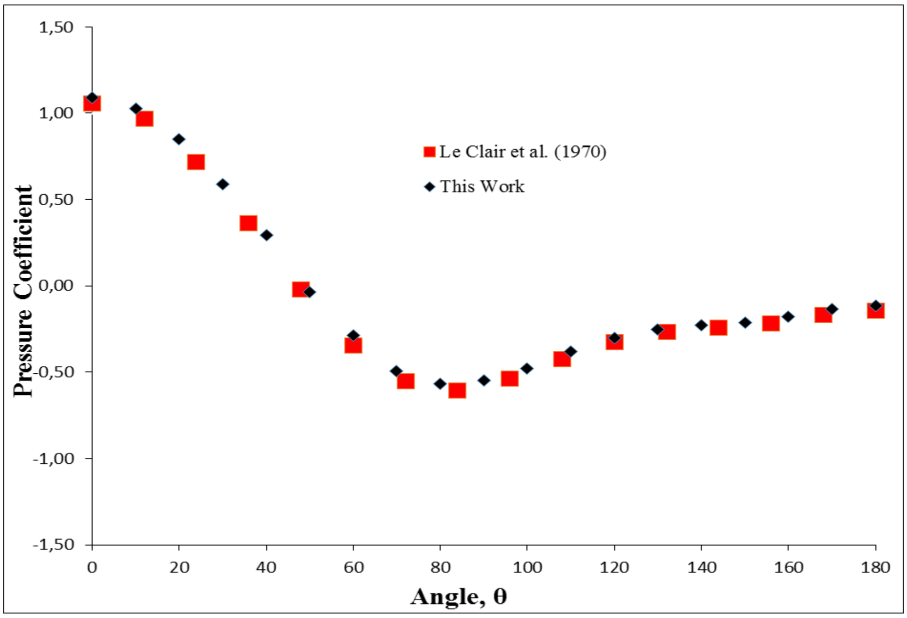

Figure 9. Pressure coefficient over the sphere surface for *Re*=200.

The results shown in Figures 8 and 9 are in good agreement with results from Le Clair et al. (1970).

4 CONCLUSIONS

In this work, a fully-explicit FEM-CBS was applied to simulate tridimensional incompressible flows and the obtained results are good in agreement with results from the literature for the benchmark problems with the expected behavior. All the results shown in this work were simulated to low and moderate Reynolds numbers, since no turbulence model was applied. This work also served as a step for learning more about this numerical method for flow simulations and then to enable an expansion of this 3D code for more complex problems.

.

Acknowledgements

The authors are grateful to CAPES and to the postgraduate program of UNESP-Ilha Solteira.

REFERENCES

Baggio, G. A. P. 2015. *Solução das Equações de Navier-Stokes e da Equação de Transporte por um Método de Elementos Finitos Estabilizado pela Técnica de Separação Baseada na Característica (CBS)*. Dissertação (Mestrado) – Universidade Estadual Paulista, Faculdade de Engenharia de Ilha Solteira, São Paulo, Brasil.

Campregher, R., Militzer, J., Mansur, S. S., Silveira Neto, A. 2009. Computations of the Flow Past a Still Sphere at Moderate Reynolds Numbers Using na Immersed Boundary Method. *Journal of the Brazilian Society of Mechanics Science & Engineering*. Vol. 31, nº4, pp 344-352.

Le Clair, B. P., Hamielec A. E., Pruppacher H. R. 1970. A Numerical Study of the Drag on a Sphere at Low and Intermediate Reynolds Numbers. *Journal of the Atmospheric Sciences*, vol. 27, pp. 308-315.

Lewis, R.W., Nithiarasu, P. and Seetharamu, K.N. 2004. *Fundamentals of the Finite Element Method for Heat and Fluid Flow*, John Wiley and Sons, Ltd, Chichester, England, 341 p.

Liu, C.B. 2005. *The Characteristic Based Split (CBS) scheme for laminar and turbulent incompressible flow simulations*, Thesis, Civil and Computational Engineering Centre, School of Engineering, University of Wales Swansea, Swansea, UK.

Nithiarasu, P., Codina, R., Zienkiewicz, O. C. 2005. The Characteristic Based Split (CBS) Scheme - a unified approach to fluid dynamics. *International Journal for Numerical Methods in Engineering*, Special issue.

Wong, K. L., Baker, A, J. A. 2002. 3D incompressible Navier–Stokes velocity–vorticity weak form finite element algorithm. *International Journal for Numerical Methods in Fluids*, v. 38, p. 99-123.

Zienkiewicz O. C., Nithiarasu, P., Codina, R., Vazquez, M., Ortiz, P. 1999. The characteristic-based-split procedure: an efficient and accurate algorithm for fluid problems. *International Journal for Numerical Methods in Fluids*; 31(1):359-396.

Zienkiewicz, O. C, Taylor, R. L, Nithiarasu, P. 2014. *The Finite Element Method vol. 3 Fluid Dynamics*, 7th edition. Butterworth and Heinemann, Oxford, 334 p.